FEMS Yeast Research, 18, 2018, foy042

doi: 10.1093/femsyr/foy042
Advance Access Publication Date: 12 April 2018
Research Article

Downloaded from https://academic.oup.com/femsyr/article-abstract/18/5/foy042/4969683 by Washington University School of Medicine Library user on 04 January 2019

RESEARCH ARTICLE

Potentiating Hsp104 activity via phosphomimetic mutations in the middle domain

Amber Tariq[1,†], JiaBei Lin[1,†], Megan M. Noll[1,†], Mariana P. Torrente[1,‡], Korrie L. Mack[1,2], Oscar Hernandez Murillo[1], Meredith E. Jackrel[1,§] and James Shorter[1,2,*,#]

[1]Department of Biochemistry and Biophysics and [2]Biochemistry and Molecular Biophysics Graduate Group, Perelman School of Medicine, University of Pennsylvania, Philadelphia, PA 19104, USA

*Corresponding author: Department of Biochemistry and Biophysics, Biochemistry and Molecular Biophysics Graduate Group, Perelman School of Medicine, University of Pennsylvania, Philadelphia, PA 19104, USA. E-mail: jshorter@pennmedicine.upenn.edu
†Co-first author.
‡Present address: Chemistry Department of Brooklyn College and Ph.D. Programs in Chemistry, Biochemistry, and Biology, Graduate Center of the City University of New York, New York, NY 10016, USA
§Present address: Department of Chemistry, Washington University, St. Louis, MO 63130, USA
One sentence summary: Potentiating Hsp104 activity via phosphomimetic mutations in the middle domain.
Editor: Brooke Bevis
#James Shorter, http://orcid.org/0000-0001-5269-8533

ABSTRACT

Hsp104 is a hexameric AAA + ATPase and protein disaggregase found in yeast, which can be potentiated via mutations in its middle domain (MD) to counter toxic phase separation by TDP-43, FUS and α-synuclein connected to devastating neurodegenerative disorders. Subtle missense mutations in the Hsp104 MD can enhance activity, indicating that post-translational modification of specific MD residues might also potentiate Hsp104. Indeed, several serine and threonine residues throughout Hsp104 can be phosphorylated in vivo. Here, we introduce phosphomimetic aspartate or glutamate residues at these positions and assess Hsp104 activity. Remarkably, phosphomimetic T499D/E and S535D/E mutations in the MD enable Hsp104 to counter TDP-43, FUS and α-synuclein aggregation and toxicity in yeast, whereas T499A/V/I and S535A do not. Moreover, Hsp104^{T499E} and Hsp104^{S535E} exhibit enhanced ATPase activity and Hsp70-independent disaggregase activity in vitro. We suggest that phosphorylation of T499 or S535 may elicit enhanced Hsp104 disaggregase activity in a reversible and regulated manner.

Keywords: disaggregase; Hsp104; neurodegeneration; ALS; PD; TDP-43

INTRODUCTION

Deleterious protein misfolding and aggregation underpin multiple devastating neurodegenerative disorders including amyotrophic lateral sclerosis (ALS), frontotemporal dementia (FTD), and Parkinson's disease (PD) (Cushman *et al.* 2010; Brettschneider *et al.* 2015; Eisele *et al.* 2015). In ~97% of ALS cases and ~45% of FTD cases, a predominantly nuclear RNA-binding protein with a prion-like domain, TDP-43, mislocalizes to cytoplasmic inclusions and becomes depleted from the nucleus in degenerating neurons (Neumann *et al.* 2006; King, Gitler and Shorter 2012; Li *et al.* 2013; Ling, Polymenidou and Cleveland 2013; Guo and Shorter 2017). However, ALS and FTD can present without TDP-43 pathology (Ling, Polymenidou and Cleveland 2013). Indeed, in ~1% of ALS cases and ~9% of FTD cases, another primarily

Received: 22 December 2017; Accepted: 10 April 2018
© FEMS 2018. All rights reserved. For permissions, please e-mail:journals.permissions@oup.com

nuclear RNA-binding protein with a prion-like domain, FUS, exhibits nuclear depletion and cytoplasmic aggregation in afflicted neurons (Kwiatkowski *et al.* 2009; Vance *et al.* 2009; March, King and Shorter 2016; Harrison and Shorter 2017). These TDP-43 and FUS pathologies likely cause a toxic gain-of-function in the cytoplasm and a toxic loss-of-function of these RNA-binding proteins in the nucleus (Harrison and Shorter 2017). Indeed, TDP-43 and FUS perform important functions in pre-mRNA splicing, transcription, translation, RNA processing, and RNA transport and together regulate the expression of thousands of human genes (Polymenidou *et al.* 2011; Lagier-Tourenne *et al.* 2012; Ling, Polymenidou and Cleveland 2013). Protein disaggregases that liberate and reactivate TDP-43 and FUS trapped in cytoplasmic inclusions and restore functional TDP-43 and FUS to the nucleus could be valuable therapeutics for ALS and FTD (Guo and Shorter 2017; Harrison and Shorter 2017).

In PD, the small, presynaptic, lipid-binding protein α-synuclein (α-syn) forms toxic oligomers and amyloids, which accumulate in cytoplasmic deposits termed Lewy bodies in degenerating dopaminergic neurons (Auluck, Caraveo and Lindquist 2010; Winner *et al.* 2011; Snead and Eliezer 2014; Abeliovich and Gitler 2016). Although the precise function of α-syn is uncertain, it likely plays important roles in synaptic vesicle trafficking (Gitler and Shorter 2007; Snead and Eliezer 2014; Abeliovich and Gitler 2016). These functions are likely perturbed via sequestration in toxic oligomers and Lewy Bodies. Thus, protein disaggregases that safely disassemble α-syn oligomers and amyloid, and recover functional α-syn could have curative properties in PD and other synucleinopathies (Shorter 2008; Snead and Eliezer 2014; Dehay *et al.* 2015).

In search of therapeutic agents, we have endeavored to tailor Hsp104, a hexameric AAA + protein disaggregase found in yeast, to safely disassemble toxic oligomers, aggregates, and amyloids connected to neurodegenerative diseases such as ALS, FTD, and PD (Shorter 2008, 2016, 2017; Jackrel and Shorter 2015, 2017). Each Hsp104 protomer contains an N-terminal domain, nucleotide-binding domain 1 (NBD1), a middle domain (MD), NBD2, and a short C-terminal domain (Fig. 1A) (Sweeny and Shorter 2016). Hsp104 assembles into asymmetric ring-like or lock-washer hexamers (Wendler *et al.* 2009; Yokom *et al.* 2016; Gates *et al.* 2017), which extract individual polypeptides from aggregated structures via partial or complete translocation across their central channel (Lum *et al.* 2004; Shorter and Lindquist 2005a; Haslberger *et al.* 2008; Lum, Niggemann and Glover 2008; Tessarz, Mogk and Bukau 2008; Castellano *et al.* 2015; Sweeny *et al.* 2015). Polypeptide translocation is driven via ratchet-like conformational changes of the hexamer that are coupled to ATP binding and hydrolysis (Yokom *et al.* 2016; Gates *et al.* 2017). Hsp104 disaggregase activity can be boosted by additional molecular chaperones, including Hsp110, Hsp70, Hsp40, Hsp42, and Hsp26 (Glover and Lindquist 1998; Cashikar, Duennwald and Lindquist 2005; Haslbeck *et al.* 2005; Shorter and Lindquist 2008; Sweeny and Shorter 2008; Shorter 2011; Duennwald, Echeverria and Shorter 2012; Sweeny *et al.* 2015; Kaimal *et al.* 2017). Hsp104 liberates diverse polypeptides trapped in insoluble phases that accumulate after stress in yeast, and thereby confers large selective advantages (Sanchez and Lindquist 1990; Parsell *et al.* 1991, 1994; Sanchez *et al.* 1992, 1993; Glover and Lindquist 1998; Shorter 2008; Wallace *et al.* 2015). Hsp104 also has a powerful amyloid-dissolvase activity (Paushkin *et al.* 1996; Shorter and Lindquist 2004, 2006; DeSantis *et al.* 2012; DeSantis and Shorter 2012b; Klaips *et al.* 2014; Sweeny *et al.* 2015; Pei *et al.* 2017; Zhao *et al.* 2017), which enables yeast to utilize and tightly regulate various prions for beneficial purposes (Chernoff *et al.* 1995; True and Lindquist 2000; True, Berlin and Lindquist 2004; Shorter and Lindquist 2005b; Halfmann, Alberti and Lindquist 2010; Tuite and Serio 2010; Newby and Lindquist 2013; Harvey, Chen and Jarosz 2017; Jarosz and Khurana 2017).

Importantly, the amyloid-dissolvase activity of Hsp104 can be turned against human neurodegenerative disease proteins. Indeed, Hsp104 dissolves diverse amyloids and toxic pre-amyloid oligomers formed by many wild-type and disease-linked mutant proteins connected to human disease, including amyloid-β, tau, α-syn, prion protein, polyglutamine and amylin (Lo Bianco *et al.* 2008; Liu *et al.* 2011; Shorter 2011; DeSantis *et al.* 2012; Duennwald, Echeverria and Shorter 2012). Moreover, Hsp104 mitigates neurodegeneration in animal models of disease (Satyal *et al.* 2000; Vacher, Garcia-Oroz and Rubinsztein 2005; Perrin *et al.* 2007; Lo Bianco *et al.* 2008; Cushman-Nick, Bonini and Shorter 2013). Despite these encouraging advances, effective amyloid dissolution can require high Hsp104 concentrations and Hsp104 is ineffective against TDP-43 and FUS (Lo Bianco *et al.* 2008; DeSantis *et al.* 2012; Jackrel and Shorter 2014a; Jackrel *et al.* 2014a). To circumvent these issues, we have engineered potentiated Hsp104 variants with enhanced disaggregase activity against TDP-43, FUS, and α-syn (Jackrel *et al.* 2014a, 2015; Jackrel and Shorter 2014a,b, 2015; Sweeny *et al.* 2015; Torrente *et al.* 2016).

Engineered Hsp104 variants with enhanced disaggregase activity successfully antagonize TDP-43, FUS, and α-syn aggregation and toxicity in yeast under conditions where Hsp104 is ineffective (Jackrel and Shorter 2014a; Jackrel *et al.* 2014a,2015). This suppression of toxicity is accompanied by relocalization of TDP-43 to the nucleus and relocalization of α-syn to the plasma membrane, indicating that protein functionality is likely restored by Hsp104 variants (Jackrel and Shorter 2014a; Jackrel *et al.* 2014a). Potentiated Hsp104 variants also dissolve TDP-43, FUS, and α-syn fibrils more effectively than Hsp104 in vitro (Jackrel and Shorter 2014a; Jackrel *et al.* 2014a). Moreover, enhanced Hsp104 variants reverse cytoplasmic aggregation and mislocalization of ALS-linked FUS in mammalian cells (Yasuda *et al.* 2017) and mitigate dopaminergic neurodegeneration caused by α-syn in a *Caenorhabditis elegans* model of PD (Jackrel *et al.* 2014a). Thus, engineered Hsp104 variants may be effective therapeutic agents to be advanced in preclinical studies.

The majority of potentiating mutations isolated to date reside in the MD of Hsp104 (Jackrel *et al.* 2014a,2015). The MD is an important autoregulatory domain of Hsp104, which encircles the disaggregase and enables interdomain communication between NBD1 and NBD2 and collaboration with Hsp70 (Cashikar *et al.* 2002; DeSantis and Shorter 2012a, 2014; Lee *et al.* 2013; Heuck *et al.* 2016; Yokom *et al.* 2016; Gates *et al.* 2017). Potentiating mutations have been found in all four helices of the MD (Jackrel *et al.* 2015). Some of these mutations may alter inter-protomer contacts between MD helix L1 and MD helix L3 or contacts between the MD and NBD1 (Heuck *et al.* 2016; Gates *et al.* 2017). Remarkably, very minor changes in primary sequence can result in enormous changes in disaggregase activity. Indeed, a single missense mutation can potentiate Hsp104 and may be as subtle as removal of a single methyl group (e.g. A503G), removal of a single methylene bridge (e.g. E469D), or addition of a single methylene bridge (e.g. V426L) (Jackrel *et al.* 2014a, 2015; Jackrel and Shorter 2015). The subtle nature of some potentiating mutations suggests that post-translational modifications of Hsp104 at specific positions in the MD or NBD1 might also potentiate activity. Indeed, several serine and threonine residues throughout Hsp104 can be phosphorylated in vivo, including T87 and S155 in the NTD, S206 and S306 in NBD1, T499 and S535 in the

Downloaded from https://academic.oup.com/femsyr/article-abstract/18/5/foy042/4969683 by Washington University School of Medicine Library user on 04 January 2019

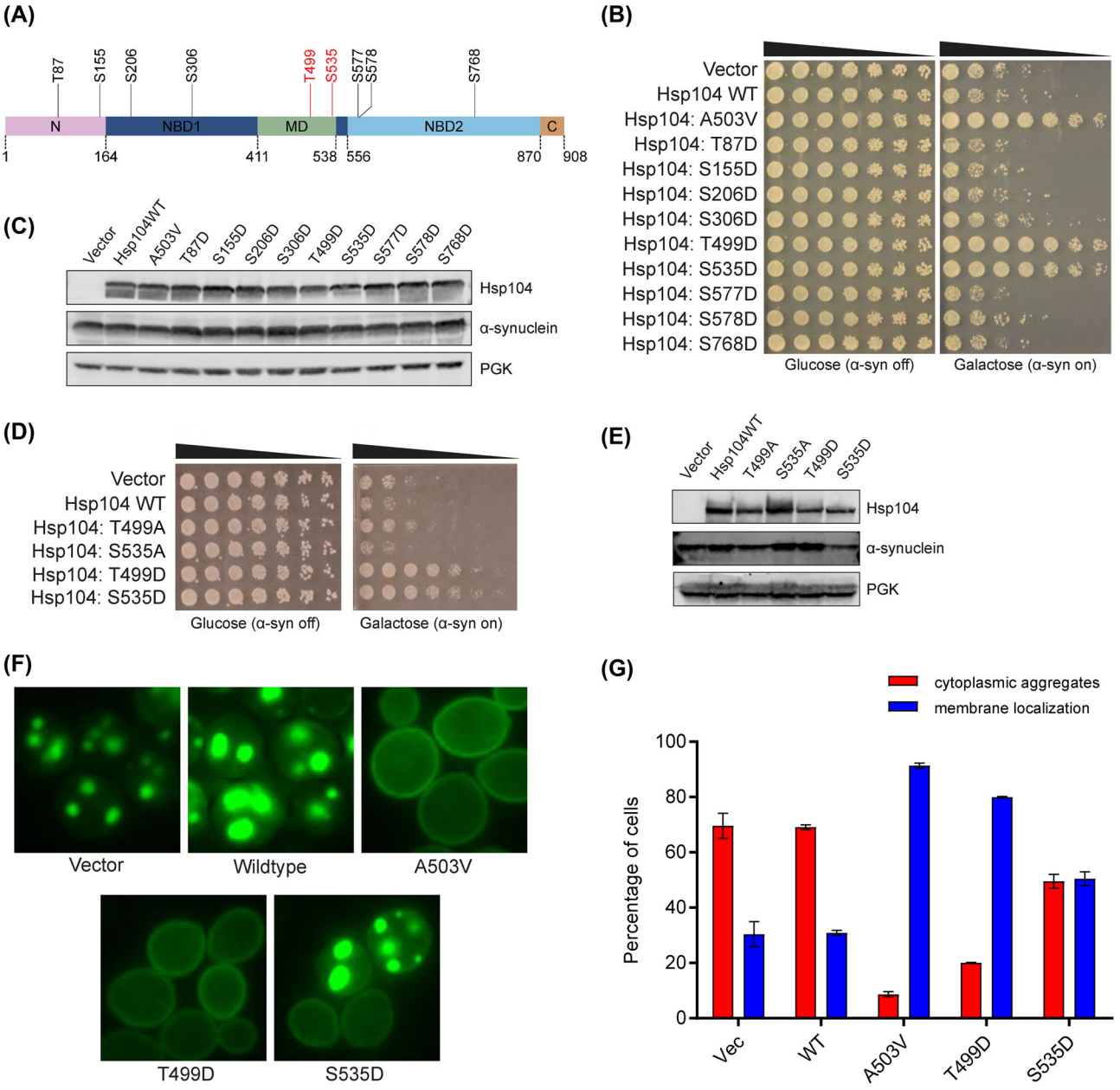

Figure 1. Hsp104^{T499D} and Hsp104^{S535D} suppress α-syn toxicity, aggregation, and mislocalization. **(A)** A map of the different domains of Hsp104 shows the location of serine and threonine residues that can be phosphorylated in vivo. The T499D and S535D potentiating mutations (denoted in red) are found in the MD (green, residues 411–538). The NTD is in pink, NBD1 is in dark blue, NBD2 is in light blue and the C-terminal domain is in brown. **(B)** Hsp104^{T499D} and Hsp104^{S535D} suppress α-syn toxicity. Phosphomimetic Hsp104 variants in the pRS416GAL-Hsp104 plasmid were transformed into W303aΔ*hsp104* yeast strains integrated with two copies of pAG303GAL-α-syn. The mutant strains were serially diluted 5-fold and spotted in duplicate onto galactose (inducing) and glucose (non-inducing) media. Two negative controls (vector, wild type) and a positive control (Hsp104^{A503V}) were spotted alongside the mutant strains. **(C)** Hsp104^{T499D} and Hsp104^{S535D} do not reduce α-syn expression. Western blots were conducted for all strains in (B) with 3-Phosphoglycerate kinase (PGK) as a loading control. The strains were induced for 8 h in galactose and lysed prior to western blotting. **(D)** Hsp104^{T499A} and Hsp104^{S535A} do not suppress α-syn toxicity. Spotting assay performed as in (B). **(E)** Hsp104^{T499A} and Hsp104^{S535A} do not reduce α-syn expression. Western blots were conducted as in (C). **(F)** Hsp104^{T499D} and Hsp104^{S535D} suppress α-syn aggregation. The potentiated variants, Hsp104^{T499D} and Hsp104^{S535D}, were transformed into α-syn-YFP yeast. The resulting strains were induced for 8 h in galactose and prepared for fluorescence microscopy. Vector, wild-type Hsp104, and the positive control Hsp104^{A503V} were prepared alongside the mutant strains. **(G)** Quantification of ~200–250 cells was performed. The cells were categorized as exhibiting either cytoplasmic aggregates or membrane localization. The graphical representation shows the means ± SEM (n = 3) for the percentage of cells in each category.

MD, and S577, S578, and S768 in NBD2 (Fig. 1A) (Albuquerque *et al.* 2008; Holt *et al.* 2009; Swaney *et al.* 2013). How these phosphorylation events affect Hsp104 activity is unknown. Here, we introduce phosphomimetic aspartate or glutamate residues at these positions and assess Hsp104 activity. Remarkably, phosphomimetic T499D/E and S535D/E mutations in the MD enable Hsp104 to effectively counter TDP-43, FUS, and α-syn aggregation and toxicity in yeast. In contrast, phosphomimetic mutations at phosphorylated positions elsewhere in Hsp104 do not potentiate Hsp104. Importantly, Hsp104^{T499E} and Hsp104^{S535E}

Downloaded from https://academic.oup.com/femsyr/article-abstract/18/5/foy042/4969683 by Washington University School of Medicine Library user on 04 January 2019

exhibit enhanced ATPase and protein-disaggregase activity. We suggest that the phosphorylation of T499 or S535 may enable enhanced Hsp104 disaggregase activity in a reversible and regulated manner.

MATERIALS AND METHODS

Yeast strains, plasmids and media

Yeast were WT W303a (*MATa, can1-100, his3-11, 15, leu2-3, 112, trp1-1, ura3-1, ade2-1*) or the isogenic strain W303aΔ*hsp104* (Jackrel *et al.* 2014a). Media was supplemented with 2% glucose, raffinose, or galactose as specified. The yeast strains W303aΔ*hsp104* 303GAL-α-syn, FUS, and TDP-43 have been previously described (Jackrel and Shorter 2014a; Jackrel *et al.* 2014a,b). QuikChange site-directed mutagenesis (Agilent, Santa Clara, CA, USA) was used to create mutations in the pRS416GAL-Hsp104 plasmid and all mutations were confirmed by DNA sequencing.

Yeast transformation and spotting assays

Yeast transformations were performed using standard polyethylene glycol and lithium acetate procedures (Gietz and Schiestl 2007). For the spotting assays, yeasts were grown to saturation in raffinose supplemented dropout media overnight at 30°C. The saturated overnight cultures were serially diluted 5-fold, and a 96-bolt replicator tool (frogger) was used to spot the strains in duplicate onto both glucose and galactose dropout plates. These plates were grown at 30°C and imaged after 72 h to assess suppression of disease-protein toxicity.

Western blotting

Transformed phosphomimetic mutants and controls were grown overnight in raffinose media. The overnight cultures were diluted to an OD of 0.3 (A_{600nm} = 0.3) and grown in galactose-supplemented media at 30°C. α-Syn samples were induced for 8 h, while FUS and TDP-43 samples were induced for 5 h. Samples were then normalized to an OD of 0.6. The pelleted cells were resuspended in 0.1 M NaOH for 5 min and then pelleted again and resuspended in 1x SDS sample buffer. The samples were then boiled and separated by SDS-PAGE (4%–20% gradient, Bio-Rad, Hercules, CA, USA), and then transferred to a PVDF membrane (Millipore). The following primary antibodies were used: anti-GFP monoclonal (Roche Applied Science, Penzburg, Germany), anti-FUS polyclonal (Bethyl Laboratories, Montgomery, TX, USA), anti-TDP-43 polyclonal (Proteintech, Rosemont, IL, USA), anti-Hsp104 polyclonal (Enzo Life Sciences, Farmingdale, NY, USA) and anti-PGK monoclonal (Invitrogen, Carlsbad, CA, USA). Blots were imaged using a LI-COR Odyssey FC Imaging system.

Toxicity assay

Phosphomimetic mutants along with applicable controls were transformed into W303aΔ*hsp104* yeast. The strains were grown overnight in raffinose dropout media at 30°C with shaking. The saturated cultures were spotted in duplicate onto two sets of SD-Ura and SGal-Ura plates. One set of plates was placed at 37°C and the other at 30°C. Both sets of plates were analyzed for toxicity after 72h.

Fluorescence microscopy

Microscopy samples were grown and induced as they were for immunoblotting. For TDP-43 samples, cells were harvested, fixed in 1 mL 70% ethanol, and immediately pelleted. The cells were then washed 3 times with cold PBS and resuspended in 15 uL of Vectashield mounting medium with 4',6-diamidino-2-phenylindole (DAPI) (Vector Laboratories, Burlingame, CA, USA). α-Syn and FUS samples were imaged live. All cells were imaged at 100x magnification using a Leica-DM-IRBE microscope. Analysis of cells was performed in ImageJ. Approximately 200–250 cells were quantified for each sample in three independent trials.

Generative REgularized models of proteINs (GREMLIN) coevolution analysis

GREMLIN coevolution analysis was performed using OPENSEQ.org web server supported by David Baker's lab (http://gremlin.bakerlab.org/) (Ovchinnikov, Kamisetty and Baker 2014). The *S. cerevisiae* Hsp104 primary sequence was used for the analysis. The Jackhammer method was used to generate the diversity multiple sequence alignment (MSA). An E-value of $1E^{-10}$ and interactions of four were chosen to control the MSA generation. Filter MSA parameters were set to remove sequences that did not cover at least 75% of query. After coverage filter, positions in the alignment that have 75% of gaps were removed.

Protein purification and biochemistry assays

Protein purification was performed as described previously (Jackrel *et al.* 2014a). ATPase activity and luciferase disaggregation and reactivation assays were performed as described (Jackrel *et al.* 2014a).

RESULTS

Hsp104^{T499D} and Hsp104^{S535D} suppress α-syn toxicity, aggregation and promote its plasma membrane localization

A number of serine and threonine residues in Hsp104 can be phosphorylated in vivo, including T87 and S155 in the NTD, S206 and S306 in NBD1, T499 and S535 in the MD, and S577, S578, and S768 in NBD2 (Fig. 1A) (Albuquerque *et al.* 2008; Holt *et al.* 2009; Swaney *et al.* 2013). To assess whether serine or threonine phosphorylation at these positions might enhance Hsp104 activity, we introduced single phosphomimetic aspartate or glutamate substitutions at these positions in Hsp104. We then determined whether these phosphomimetic Hsp104 variants could antagonize α-syn toxicity in yeast. Upon expression from the inducible galactose promoter, α-syn accumulates in cytoplasmic aggregates and is toxic to yeast thereby recapitulating the phenotype of degenerating dopaminergic neurons in PD patients (Outeiro and Lindquist 2003). This yeast model of α-syn aggregation and toxicity has been tremendously valuable in identifying novel genetic and small-molecule suppressors of α-syn toxicity, which have translated to worm, fly, mouse, and patient-derived neuronal models of PD (Cooper *et al.* 2006; Gitler *et al.* 2008, 2009; Su *et al.* 2010; Chung *et al.* 2013; Tardiff and Lindquist 2013; Tardiff *et al.* 2013; Caraveo *et al.* 2014, 2017; Jackrel *et al.* 2014a; Khurana *et al.* 2017).

α-Syn overexpression is toxic to yeast (Fig. 1B) and is an established cause of PD (Singleton *et al.* 2003). This α-syn toxicity cannot be buffered by wild-type Hsp104 (Fig. 1B). Likewise, the phosphomimetic aspartate variants Hsp104^{T87D}, Hsp104^{S155D}, Hsp104^{S206D}, Hsp104^{S306D}, Hsp104^{S577D}, Hsp104^{S578D}, and Hsp104^{S768D} were unable to rescue α-syn toxicity despite

Downloaded from https://academic.oup.com/femsyr/article-abstract/18/5/foy042/4969683 by Washington University School of Medicine Library user on 04 January 2019

being robustly expressed (Fig. 1B and C). In contrast, Hsp104^{T499D} and Hsp104^{S535D} strongly suppressed α-syn toxicity to a level similar to the canonical potentiated Hsp104 variant, Hsp104^{A503V} (Fig. 1B). This rescue was achieved without any reduction in α-syn expression (Fig. 1C). Very similar results were obtained with phosphomimetic glutamate variants. Thus, only Hsp104^{T499E} and Hsp104^{S535E} rescued α-syn toxicity (data not shown). Altogether, we find phosphomimetic mutations at T499 or S535 in the MD potentiate Hsp104 activity, whereas single phosphomimetic mutations at T87 or S155 in the NTD, or S206 or S306 in NBD1, or S577, S578, or S768 in NBD2 do not.

Several positions in the MD can be mutated to diverse amino acids and confer potentiated Hsp104 activity (Jackrel *et al.* 2014a). For example, A503 in helix L3 of the MD can be mutated to *any* amino acid, except proline, and enable Hsp104 to strongly suppress α-syn, FUS, and TDP-43 toxicity (Jackrel *et al.* 2014a). To confirm that enhanced Hsp104 activity was due to the phosphomimetic mutation at T499 or S535 rather than a general effect of any mutation, we generated the T499A and S535A variants. Unlike Hsp104^{T499D} or Hsp104^{S535D}, neither Hsp104^{T499A} nor Hsp104^{S535A} rescued α-syn toxicity despite robust expression (Fig. 1D and E). Thus, unlike A503, not any mutation at T499 or S535 potentiates Hsp104 activity. Indeed, we also assessed T499I, a mutation that when combined with G217S causes Hsp104 to be toxic (Schirmer *et al.* 2004). Hsp104^{T499I} exhibits mildly reduced ATPase activity in vitro, but confers thermotolerance in vivo (Schirmer *et al.* 2004). Like Hsp104^{T499A}, Hsp104^{T499I} was unable to rescue α-syn toxicity (data not shown). Moreover, we have previously shown that Hsp104^{T499V} does not rescue α-syn toxicity (Jackrel *et al.* 2014a). Thus, only select missense mutations at the T499 position confer potentiated activity.

α-Syn accumulates in cytoplasmic aggregated structures in yeast that are not affected by expression of Hsp104 (Fig. 1F and G). Indeed, ~70% of cells present with cytoplasmic α-syn foci in the vector control or in the presence of Hsp104 (Fig. 1F). In contrast, the potentiated variant, Hsp104^{A503V}, antagonizes formation of cytoplasmic α-syn foci and enables α-syn to localize to the plasma membrane in ~90% of cells (Fig. 1F and G). The MD phosphomimetic variants, Hsp104^{T499D} and Hsp104^{S535D}, also suppressed the formation of cytoplasmic α-syn aggregates and enabled α-syn localization to the plasma membrane in ~80% and ~50% of cells, respectively (Fig. 1F and G). Thus, Hsp104^{T499D} and Hsp104^{S535D} are not as effective as Hsp104^{A503V} in suppressing cytoplasmic α-syn aggregation. Regardless, the level of protection against cytoplasmic α-syn aggregation conferred by Hsp104^{T499D} and Hsp104^{S535D} is sufficient to potently mitigate α-syn toxicity (Fig. 1B and D).

Hsp104^{T499D} and Hsp104^{S535D} suppress TDP-43 toxicity, aggregation and promote its nuclear localization

Next, we assessed the same single phosphomimetic aspartate or glutamate Hsp104 variants against TDP-43 aggregation and toxicity in yeast. TDP-43 is a mostly nuclear protein that shuttles between the nucleus and cytoplasm, but aggregates and mislocalizes to the cytoplasm of degenerating motor neurons in ALS and cortical neurons in FTD (Guo and Shorter 2017). Overexpression of TDP-43 in yeast replicates these phenotypes of cytoplasmic aggregation and toxicity (Johnson *et al.* 2008, 2009). Indeed, TDP-43 overexpression is connected to FTD (Gitcho *et al.* 2009). This yeast model of TDP-43 aggregation and toxicity has empowered the discovery of key genetic and small-molecule modifiers of TDP-43 toxicity, which have translated to fly, mouse, and neuronal models of ALS/FTD (Elden *et al.* 2010; Armakola *et al.* 2012; Tardiff *et al.* 2012; Kim *et al.* 2014; Jackrel *et al.* 2014a; Becker *et al.* 2017). Indeed, this yeast model sparked the discovery of intermediate-length, polyglutamine expansions (~27–33 glutamines) in ataxin 2 as a common risk factor for ALS (Elden *et al.* 2010; Lee *et al.* 2011a,b; Yu *et al.* 2011; Auburger *et al.* 2017).

TDP-43 toxicity was not rescued by Hsp104 or by any of the aspartate or glutamate phosphomimetic variants in the NTD, NBD1, or NBD2 (Fig. 2A). In contrast, the MD phosphomimetic variants, Hsp104^{T499D} and Hsp104^{S535D}, mitigated TDP-43 toxicity (Fig. 2A). Hsp104^{T499E} and Hsp104^{S535E} also rescued TDP-43 toxicity (data not shown). Rescue of TDP-43 toxicity by Hsp104^{T499D} and Hsp104^{S535D} was similar to that achieved by Hsp104^{A503V} and was not due to gross reductions in TDP-43 expression levels (Fig. 2A and B). In contrast, Hsp104^{T499A}, Hsp104^{T499I}, Hsp104^{T499V} and Hsp104^{S535A} did not rescue TDP-43 toxicity (Fig. 2C and D; data not shown) (Jackrel *et al.* 2014a). Thus, phosphomimetic mutations at T499 or S535 enhanced Hsp104 activity against TDP-43, whereas alanine, valine or isoleucine substitutions at T499 or alanine substitution at S535 did not.

We determined that Hsp104^{T499D} and Hsp104^{S535D} also suppressed TDP-43 aggregation and mislocalization (Fig. 2E and F). In yeast expressing Hsp104 or the vector control, TDP-43 was found in the nucleus in ~35% of cells, whereas ~65% had cytoplasmic TDP-43 aggregates (Fig. 2E and F). Conversely, in yeast cells expressing Hsp104^{T499D} or Hsp104^{S535D} TDP-43 was found in the nucleus in ~65% of cells, whereas ~35% had cytoplasmic TDP-43 aggregates (Fig. 2E and F). Collectively, these findings establish that Hsp104^{T499D} and Hsp104^{S535D} are potent suppressors of TDP-43 aggregation and toxicity. Importantly, Hsp104^{T499D} and Hsp104^{S535D} also restore TDP-43 localization to the nucleus.

Hsp104^{T499D} and Hsp104^{S535D} suppress FUS toxicity and aggregation

We next assessed phosphomimetic Hsp104 variants against FUS proteotoxicity. FUS overexpression in yeast induces cytoplasmic FUS aggregation and toxicity, thereby mimicking events in degenerating neurons in ALS or FTD with FUS pathology (Ju *et al.* 2011; Sun *et al.* 2011; Harrison and Shorter 2017). Moreover, elevated FUS expression is also connected to neurodegenerative disease (Sabatelli *et al.* 2013; Dini Modigliani *et al.* 2014). This yeast model of FUS proteinopathies has enabled discovery of several genetic modifiers of FUS toxicity, which have translated to fly, mammalian cell and neuronal models of ALS and FTD (Sun *et al.* 2011; Daigle *et al.* 2013; Jackrel *et al.* 2014a; Barmada *et al.* 2015; Daigle *et al.* 2016; Yasuda *et al.* 2017).

As with α-syn and TDP-43, FUS toxicity was not buffered by wild-type Hsp104 or by any of the aspartate or glutamate phosphomimetic variants in the NTD, NBD1 or NBD2 (Fig. 3A). However, Hsp104^{T499D} and Hsp104^{S535D} strongly mitigated FUS toxicity and were just as effective as Hsp104^{A503V} (Fig. 3A). These potentiated variants also mildly reduced FUS protein levels and this effect was most pronounced for Hsp104^{A503V} (Fig. 3B). Hsp104^{T499E} and Hsp104^{S535E} also strongly rescued FUS toxicity (data not shown). In contrast, Hsp104^{T499A}, Hsp104^{T499I}, Hsp104^{T499V} and Hsp104^{S535A} did not rescue FUS toxicity (Fig. 3C and D; data not shown) (Jackrel *et al.* 2014a). Thus, rescue of FUS toxicity was enabled by phosphomimetic mutations at T499 or S535, whereas other substitutions at T499 or S535 explored here were ineffective.

Hsp104^{T499D} and Hsp104^{S535D} also reduced cytoplasmic FUS aggregation in yeast (Fig. 3E and F). Indeed, over 80% of cells

Downloaded from https://academic.oup.com/femsyr/article-abstract/18/5/foy042/4969683 by Washington University School of Medicine Library user on 04 January 2019

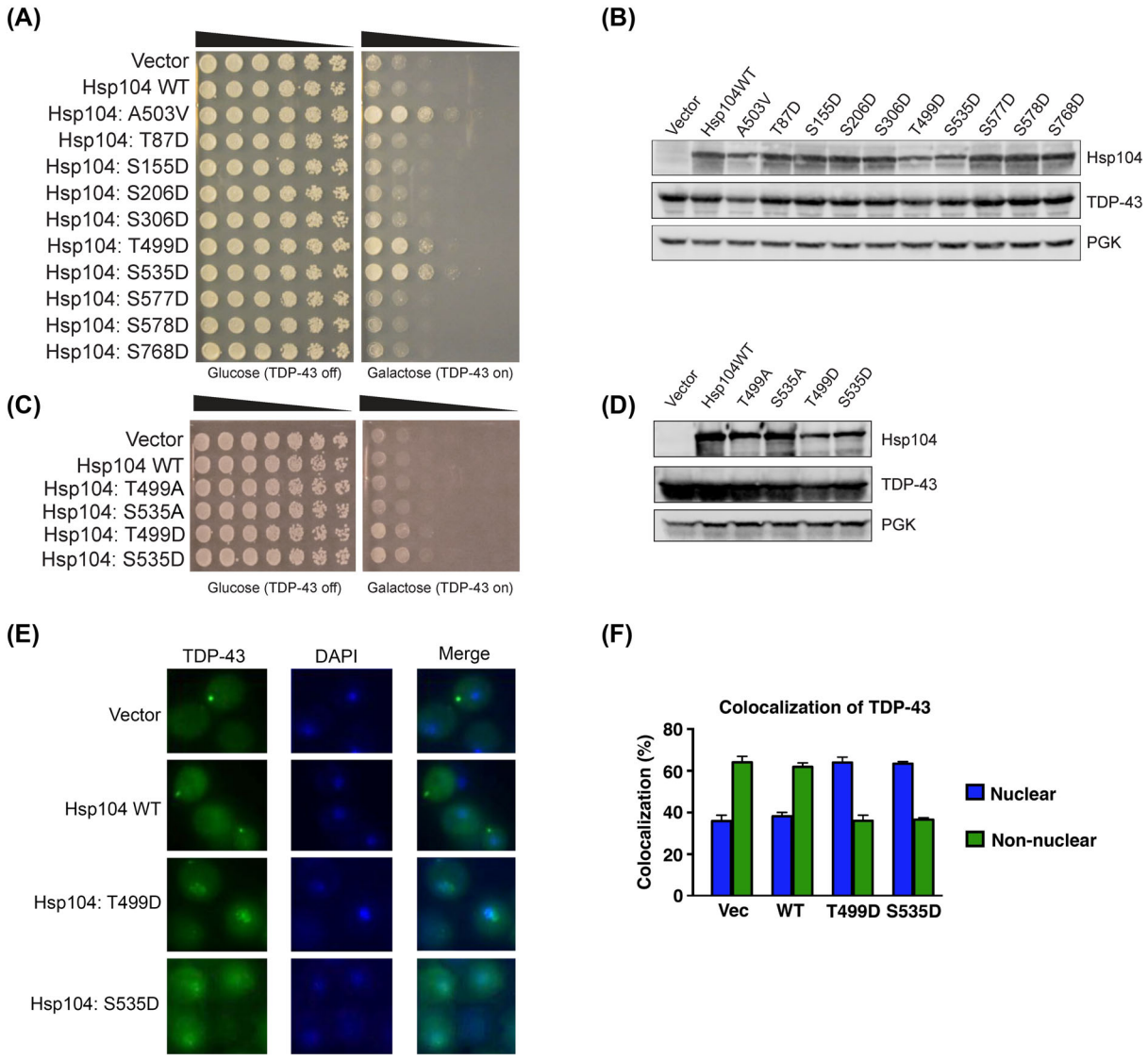

Figure 2. Hsp104^{T499D} and Hsp104^{S535D} antagonize TDP-43 aggregation, toxicity and restore TDP-43 to the nucleus. **(A)** Hsp104^{T499D} and Hsp104^{S535D} antagonize TDP-43 toxicity. Phosphomimetic variants in the pRS416GAL-Hsp104 plasmid were transformed into W303a*Δhsp104* yeast strains integrated with pAG303GAL-TDP-43. The mutant strains were serially diluted 5-fold and spotted in duplicate onto galactose (inducing) and glucose (non-inducing) media. Two negative controls (vector, wild type) and a positive control (Hsp104^{A503V}) were spotted alongside the mutant strains. **(B)** Hsp104^{T499D} and Hsp104^{S535D} do not grossly reduce TDP-43 expression. Western blots were conducted for all strains in (A) with 3-Phosphoglycerate kinase (PGK) as a loading control. The strains were induced for 5 h in galactose and lysed prior to western blotting. **(C)** Hsp104^{T499A} and Hsp104^{S535A} do not suppress TDP-43 toxicity. Spotting assay performed as in (A). **(D)** Hsp104^{T499A} and Hsp104^{S535A} do not reduce TDP-43 expression. Western blots were conducted as in (B). **(E)** Hsp104^{T499D} and Hsp104^{S535D} suppress cytoplasmic TDP-43 aggregation and promote nuclear TDP-43 localization in yeast. Fluorescence microscopy of cells coexpressing fluorescently tagged TDP-43 and the Hsp104 variants was performed. Strains were induced for 5 h in galactose, fixed, and stained with DAPI (blue) to visualize nuclei. **(F)** TDP-43 localization was quantified by counting the number of cells containing colocalized nuclear staining. 200–250 cells per treatment were counted for each trial, and the values represent means ± SEM (n = 3).

harbor cytoplasmic FUS aggregates in the vector and Hsp104 controls, whereas ~55% and ~40% of cells had no cytoplasmic FUS aggregates in cells expressing Hsp104^{T499D} and Hsp104^{S535D} respectively (Fig. 3F). The reduction of cytoplasmic FUS aggregation by Hsp104^{T499D} and Hsp104^{S535D} was not as pronounced as that observed with Hsp104^{A503V} where ~75% of cells had no cytoplasmic FUS aggregates (Fig. 3F). Nonetheless, Hsp104^{T499D} and Hsp104^{S535D} mitigated FUS toxicity just as effectively as Hsp104^{A503V}. Taken together, these observations indicate that Hsp104^{T499D} and Hsp104^{S535D} potently suppress FUS aggregation and toxicity.

Hsp104$^{T499D/E}$ but not Hsp104$^{S535D/E}$ reduces yeast growth at 37°C

Potentiated Hsp104 variants with mutations in the MD such as Hsp104^{A503V} can confer a temperature-sensitive growth defect whereby yeast grow normally at 30°C but exhibit attenuated growth at 37°C (Fig. 4) (Jackrel and Shorter 2014a,b; Jackrel *et al.* 2014a). This toxicity at 37°C likely reflects off-target effects such as promiscuous binding and unfolding of essential proteins (Schirmer *et al.* 2004; Jackrel and Shorter 2014a,b; Jackrel *et al.* 2014a). Thus, we assessed whether Hsp104^{T499D},

Downloaded from https://academic.oup.com/femsyr/article-abstract/18/5/foy042/4969683 by Washington University School of Medicine Library user on 04 January 2019

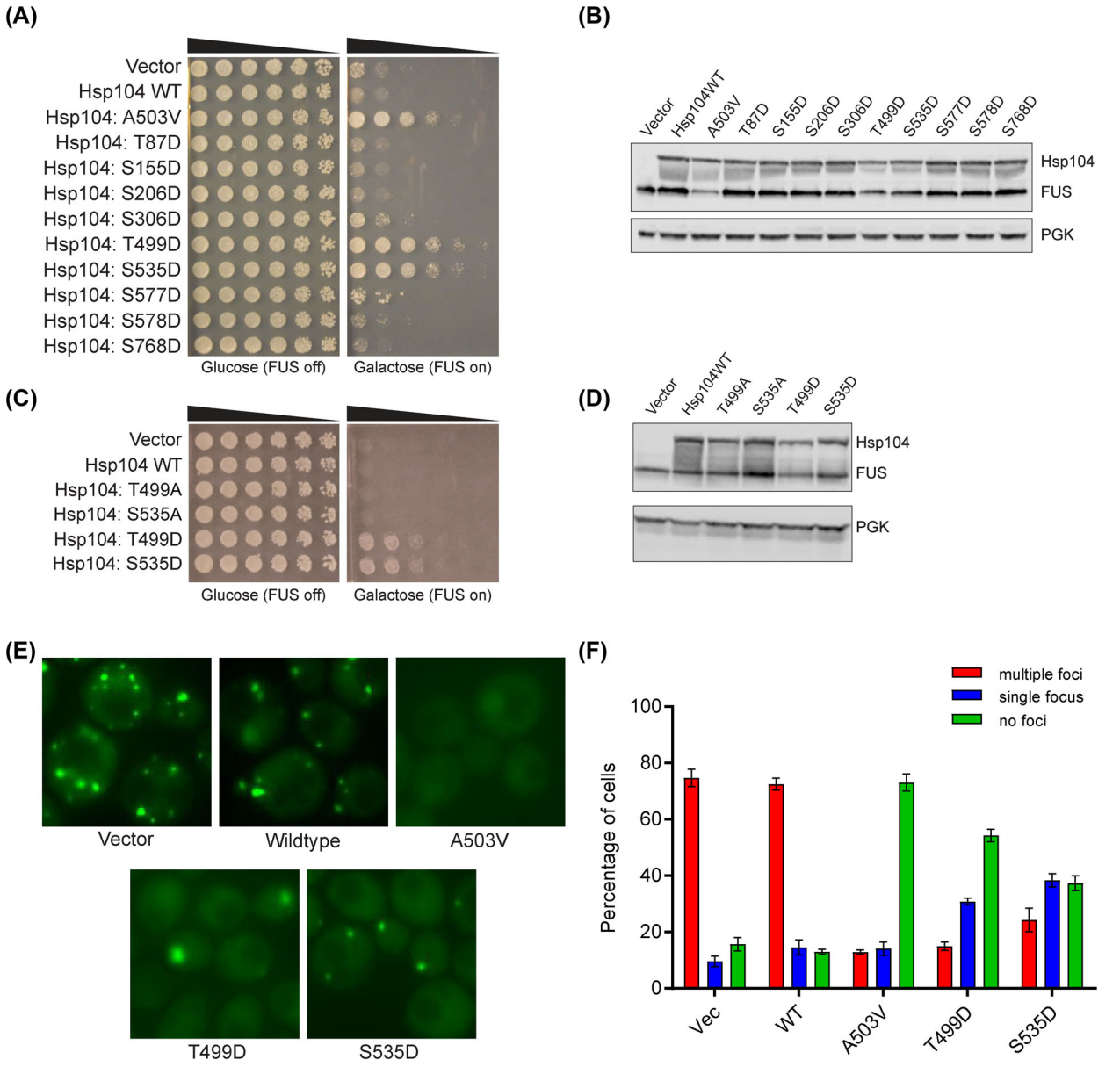

Figure 3. Hsp104^{T499D} and Hsp104^{S535D} antagonize FUS toxicity and aggregation. **(A)** Hsp104^{T499D} and Hsp104^{S535D} antagonize FUS toxicity. Phosphomimetic variants in the pRS416GAL-Hsp104 plasmid were transformed into W303a*Δhsp104* yeast strains integrated with pAG303GAL-FUS. The mutant strains were serially diluted 5-fold and spotted in duplicate onto galactose (inducing) and glucose (non-inducing) media. Two negative controls (vector, wild type) and a positive control (Hsp104^{A503V}) were spotted alongside the mutant strains. **(B)** Hsp104^{T499D} and Hsp104^{S535D} do not grossly reduce FUS expression. Western blots were conducted for all strains in (A) with 3-Phosphoglycerate kinase (PGK) as a loading control. The strains were induced for 5 h in galactose and lysed prior to western blotting. **(C)** Hsp104^{T499A} and Hsp104^{S535A} do not suppress FUS toxicity. Spotting assay performed as in (A). **(D)** Hsp104^{T499A} and Hsp104^{S535A} do not reduce FUS expression. Western blots were conducted as in (B). **(E)** Hsp104^{T499D} and Hsp104^{S535D} suppress FUS aggregation in yeast. The potentiated mutations T499D and S535D were transformed into FUS GFP-tagged yeast. The resulting strains were induced for 5 h in galactose and prepared for fluorescence microscopy. Vector, wild type, and the positive control Hsp104^{A503V} were prepared alongside the mutant strains. **(F)** Quantification of approximately 200–250 cells was performed. The cells were categorized as containing multiple foci, a single focus, or no foci. The graphical representation shows the means ± SEM (n = 3) for the percentage of cells in each category.

Hsp104^{T499E}, Hsp104^{S535D} or Hsp104^{S535E} might also confer this phenotype. None of the variants were toxic at 30°C (Fig. 4). In contrast, expression of Hsp104^{T499D} or Hsp104^{T499E} was toxic at 37°C, indicating that these variants have off-target effects (Fig. 4). Hsp104^{T499D} and Hsp104^{T499E} toxicity at 37°C was similar to Hsp104^{A503V} (Fig. 4). Despite these off-target effects in the absence of disease protein, Hsp104^{T499D} and Hsp104^{T499E} potently rescue α-syn, TDP-43, and FUS toxicity. In contrast, Hsp104^{S535D} and Hsp104^{S535E} were not toxic to yeast at 37°C and resembled wild-type Hsp104 (Fig. 4). Thus, Hsp104^{S535D} and Hsp104^{S535E} exhibit potentiated activity but minimal off-target toxicity, which are attractive features for therapeutic protein disaggregases to be advanced to preclinical studies.

Location of T499 and S535 in Hsp104 hexamers

Next, we mapped the potentiating phosphomimetic mutations onto the structure of Hsp104 hexamers bound to ADP

Downloaded from https://academic.oup.com/femsyr/article-abstract/18/5/foy042/4969683 by Washington University School of Medicine Library user on 04 January 2019

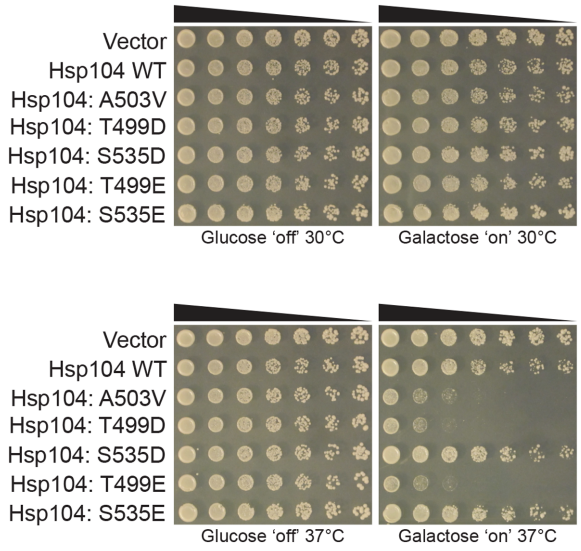

Figure 4. $Hsp104^{T499D/E}$ but not $Hsp104^{S535D/E}$ reduces yeast growth at 37°C. Hsp104 variants were expressed in the 416GAL vector in Δ*hsp104* yeast in the absence of any disease protein. The strains were serially diluted 5-fold and spotted in duplicate onto glucose (non-inducing) media at 30°C or galactose (inducing) media at 30°C or 37°C.

(Gates *et al.* 2017). T499 is a poorly conserved residue and is typically a leucine or a large aromatic residue in other homologues (Fig. 5A). T499 is found at the start of helix L3 in the MD and is anticipated to be readily accessible to kinases and phosphatases (Fig. 5B) (Yokom *et al.* 2016; Gates *et al.* 2017). Generative REgularized ModeLs of proteINs (GREMLIN) analysis of Hsp104 suggest that T499 interacts and coevolves with A503 in helix L3 (Fig. 5C) (Ovchinnikov, Kamisetty and Baker 2014). Indeed, the structure of Hsp104 hexamers in the presence of ADP suggests that T499 interacts with A503 in the same protomer via a backbone hydrogen bond (Fig. 5C) (Gates *et al.* 2017). Mutation of A503 to any amino acid except proline potentiates Hsp104 (Jackrel *et al.* 2014a), which may be due to disruption of the interaction with residue T499. Likewise, mutation of T499 to aspartate or glutamate, but not alanine, valine, or isoleucine likely also perturbs the interaction with A503 leading to potentiated activity. T499 may also make an intramolecular contact with E494 in helix L2 of the MD in protomer 4 (Gates *et al.* 2017). Interestingly, T499 also contacts MD residues V426 and K429 in the neighboring protomer (Fig. 5C). Mutations at V426 can also potentiate Hsp104 activity (Jackrel *et al.* 2014a,2015). Thus, remodeling this network of interactions within the MD and between MDs in adjacent protomers likely yields potentiated activity.

Like T499, S535 is a poorly conserved residue and is typically proline or arginine in other homologues (Fig. 5A). S535 resides in the linker between helix L4 in the MD and the C-terminal remainder of NBD1 and is likely accessible to kinases and phosphatases (Fig. 5B) (Yokom *et al.* 2016; Gates *et al.* 2017). Intriguingly, S535 makes intraprotomer contacts with E469 in helix L2 of the MD (Fig. 5D) (Gates *et al.* 2017). S535D and E469D potentiate Hsp104 activity perhaps due to alteration of this intraprotomer MD contact (Jackrel *et al.* 2015).

$Hsp104^{T499E}$ and $Hsp104^{S535E}$ exhibit enhanced ATPase and protein-disaggregase activity

Next, we purified $Hsp104^{T499E}$ and $Hsp104^{S535E}$ and assessed how their biochemical activity compared to Hsp104. First, we established that these phosphomimetic MD variants display elevated ATPase activity (Fig. 6A). $Hsp104^{T499E}$ exhibited ATPase activity ~4-fold higher than Hsp104, whereas $Hsp104^{S535E}$ was ~2-fold higher (Fig. 6A). Second, we tested the protein disaggregation and reactivation activity of $Hsp104^{T499E}$ and $Hsp104^{S535E}$ variants using denatured luciferase aggregates as a model substrate (Glover and Lindquist 1998). While Hsp104 requires Hsp70 and Hsp40 for luciferase reactivation (Glover and Lindquist 1998), $Hsp104^{T499E}$ and $Hsp104^{S535E}$ do not (Fig. 6B). In the absence of Hsp70 and Hsp40, $Hsp104^{S535E}$ was slightly less active than Hsp104 with Hsp70 and Hsp40, whereas $Hsp104^{T499E}$ was ~6-fold more active (Fig. 6B). The addition of Hsp70 and Hsp40 to $Hsp104^{S535E}$ variants increased luciferase reactivation by ~6-fold, whereas $Hsp104^{T499E}$ was stimulated only slightly further (Fig. 6B). $Hsp104^{T499E}$ is almost fully active without Hsp70 and Hsp40 (Fig. 6B). In contrast, $Hsp104^{S535E}$ was greatly stimulated by Hsp70 and Hsp40 (Fig. 6B). These observations indicate differences in the mechanism of potentiation by T499E and S535E, which likely reflects the rearrangement of different structural contacts (Fig. 5C and D). Nonetheless, the potentiating T499E and S535E mutations increase disaggregase activity in the absence or presence of Hsp70 and Hsp40.

DISCUSSION

The subtle nature of some potentiating mutations in Hsp104 led us to hypothesize that post-translational modifications of Hsp104 at specific positions in the MD might also potentiate activity. Indeed, several serine and threonine residues throughout Hsp104 can be phosphorylated in vivo (Albuquerque *et al.* 2008; Holt *et al.* 2009; Swaney *et al.* 2013). Here, we have introduced phosphomimetic aspartate or glutamate residues at these positions and assessed Hsp104 activity. Phosphomimetic mutations at T87 and S155 in the NTD, S206 and S306 in NBD1, or S577, S578 and S768 in NBD2 did not enhance Hsp104 activity. Remarkably, phosphomimetic mutations at two positions in the MD, T499 and S535, enabled Hsp104 to rescue TDP-43, FUS, and α-syn aggregation and toxicity in yeast. Moreover, $Hsp104^{T499E}$ and $Hsp104^{S535E}$ exhibit enhanced ATPase activity and protein-disaggregase activity in vitro. We suggest that phosphorylation of T499 or S535 may enable enhanced Hsp104 disaggregase activity in a reversible and regulated manner. Thus, enhanced disaggregase activity could be unleashed and restrained at specific locations or in response to specific environmental cues in vivo. Understanding this regulation could also inform strategies to engineer transient bursts of enhanced disaggregase activity in therapeutic settings.

How do the T499D/E and S535D/E mutations potentiate Hsp104? Mutation to a negatively charged residue is important as alanine, valine or isoleucine at T499 do not enhance activity. Likewise, alanine at S535 does not potentiate Hsp104. Thus, T499 and S535 are not like A503, where any amino acid aside from alanine or proline elicits elevated disaggregase activity. Interestingly, T499 lies in helix L3 of the MD and has coevolved and interacts with A503. Mutation of T499 to aspartate or glutamate likely alters interactions with A503 in the same protomer, but also with E494 in helix L2 of the same protomer (in protomer 4) and V426 in helix L1 of the MD in the adjacent protomer (Gates *et al.* 2017). Remodeling these interactions by T499D/E yields a potentiated Hsp104 variant with highly elevated disaggregase activity even in the absence of Hsp70. However, $Hsp104^{T499D/E}$ also exhibits off-target toxicity, which is disadvantageous for further development as a therapeutic disaggregase. In contrast,

Downloaded from https://academic.oup.com/femsyr/article-abstract/18/5/foy042/4969683 by Washington University School of Medicine Library user on 04 January 2019

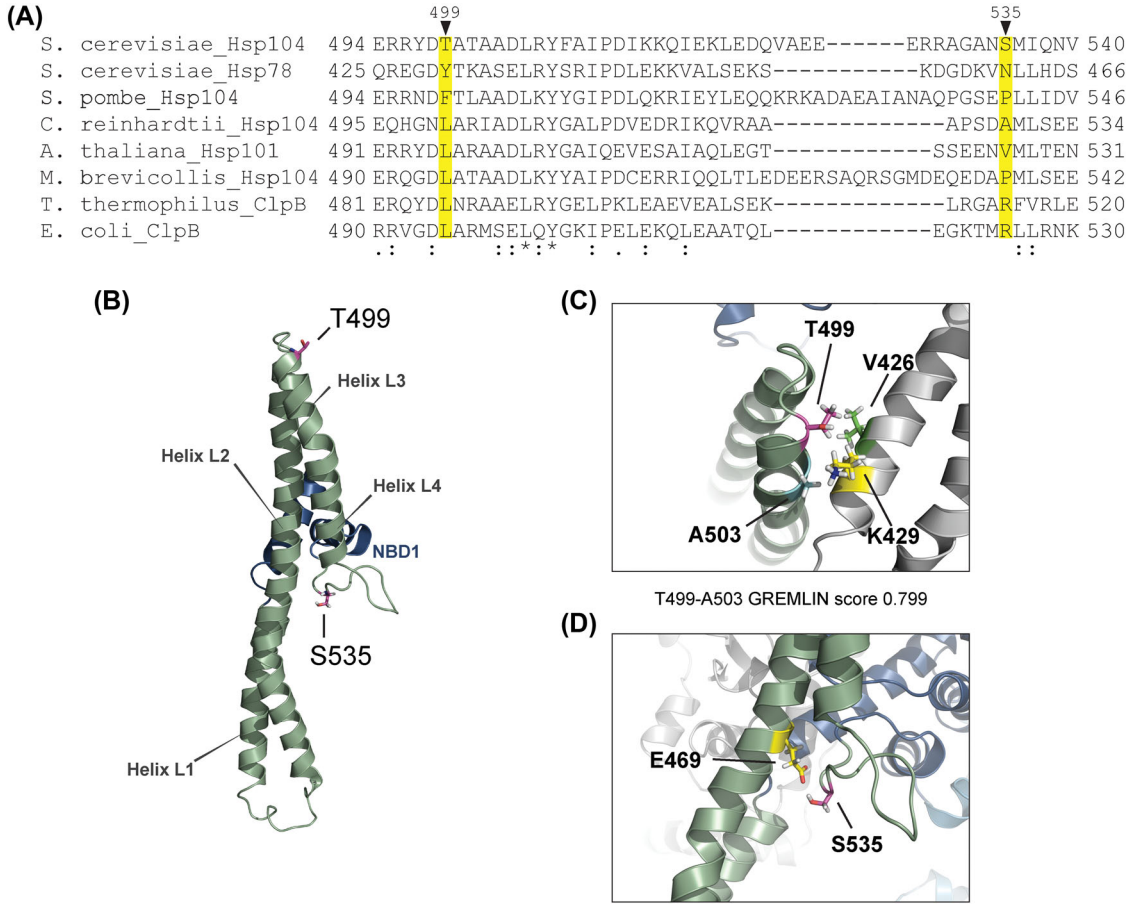

Figure 5. Location of potentiating phosphomimetic MD mutations in Hsp104. **(A)** Clustal Omega alignment of a portion (residues 494–540) of the MD/NBD1 from *Saccharomyces cerevisiae* Hsp104 with *S. cerevisiae* Hsp78, *Schizosaccharomyces pombe* Hsp104, *Chlamydomonas reinhardtii* Hsp104, *Arabidopsis thaliana* Hsp101, *Monosiga brevicollis* Hsp104, *Thermus thermophilus* ClpB, and *Escherichia coli* ClpB. T499 and S535 are indicated with arrowheads and highlighted in yellow. Consensus symbols: '∗' denotes fully conserved residue, ':' denotes conservation of residues with strong similarity, '.' indicates the conservation of residues with weak similarity. **(B)** Homology model of the MD (green) and a portion of the small domain of NBD1 (dark blue) of Hsp104, where T499 and S535 side chains are shown as sticks. T499 is found in helix L3 and S535 is in the linker between helix L4 and the C-terminal portion of the small domain of NBD1 (dark blue). **(C)** View of protomers 3 (green) and 4 (grey) of Hsp104 bound to ADP (Gates *et al.* 2017) showing the positions of T499 and A503 in helix L3 of the MD of protomer 3 and V426 and K229 in helix L1 of protomer 4. The GREMLIN score for the interaction between T499 and A503 is indicated. **(D)** View of protomer 3 of Hsp104 bound to ADP (Gates *et al.* 2017) showing the positions of S535 in the linker between helix L4 of the MD and NDB1 and E469 in helix L2 of the MD of the same protomer.

Hsp104$^{S535D/E}$ is not toxic. Hsp104^{S535E} disaggregase activity is not as elevated as Hsp104^{T499E} in the absence or presence of Hsp70, but is substantially higher than Hsp104. S535D/E likely disrupts an intraprotomer interaction with E469 in helix L2 of the MD. Hsp104^{E469D} is also an enhanced Hsp104 variant, which like Hsp104$^{S535D/E}$ exhibits reduced off-target toxicity (Jackrel *et al.* 2015). Thus, Hsp104$^{S535D/E}$ and Hsp104^{E469D} are interesting variants to advance in preclinical studies as they potently rescue proteotoxicity with minimal side effects.

Under what conditions are T499 and S535 phosphorylated in vivo? One study found that Hsp104 may be phosphorylated at T499 and S535 under conditions of DNA damage stress (Albuquerque *et al.* 2008). These observations raise the possibility that Hsp104 might get phosphorylated at T499 or S535 as part of a stress response to elicit enhanced disaggregase activity, which is cytoprotective. Once the stress has passed, dephosphorylation of T499 or S535 would restore Hsp104 activity to basal levels. In this way, yeast may utilize phosphorylation of T499 or S535 to unleash enhanced Hsp104 disaggregase activity exactly when or where it is needed in a reversible and regulated manner.

Curiously, T499 and S535 are not very well conserved residues. Indeed, of the 4950 Hsp104 species variants assessed in our GREMLIN analysis, ∼1.7% had T at position 499. Indeed, L, Y or F were most commonly found at position 499 (Fig. 5A). Likewise, only ∼13% of Hsp104 species variants had S at position 535 (Fig. 5A). At this position, P or R was the most commonly found residue. Thus, this potential method of Hsp104 regulation via phosphorylation of T499 or S535 may be idiosyncratic to a restricted number of species. However, position 499 is frequently tyrosine in ∼16% of species, and thus could be regulated in a similar manner via tyrosine phosphorylation. Further studies are needed to reveal under what exact conditions Hsp104 is phosphorylated at T499 or S535 in yeast. The identity of Hsp104 kinases and phosphatases also needs to be delineated. Indeed, it will be of great interest to reconstitute the regulation of potentiated Hsp104 disaggregase activity in vitro via the addition of defined kinases and phosphatases. Other post-translational modifications may also unleash enhanced Hsp104 activity in a regulated manner. For example, the MD of Hsp104 can be modified via ubiquitylation, succinylation, and acetylation, which

Downloaded from https://academic.oup.com/femsyr/article-abstract/18/5/foy042/4969683 by Washington University School of Medicine Library user on 04 January 2019

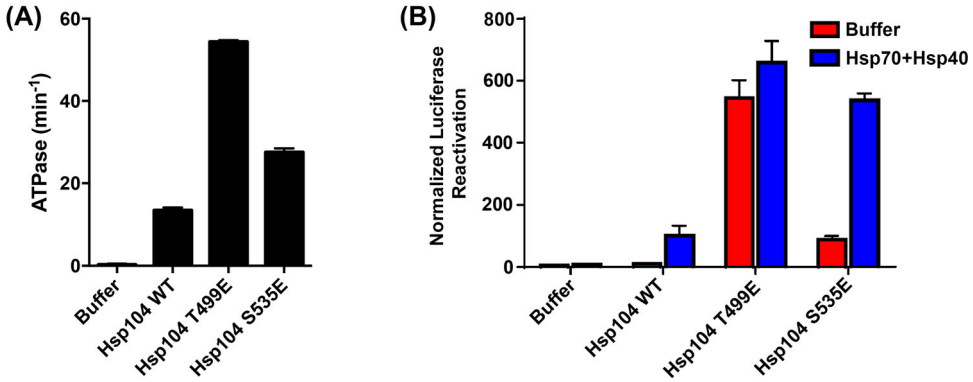

Figure 6. Hsp104^{T499E} and Hsp104^{S535E} exhibit enhanced ATPase and protein-disaggregase activity. **(A)** Hsp104^{T499E} and Hsp104^{S535E} exhibit elevated ATPase activity. Values represent means ± SD (n = 2). **(B)** Hsp104^{T499E} and Hsp104^{S535E} exhibit elevated disaggregase activity. Luciferase aggregates were incubated with Hsp104 variant (0.167 μM) plus ATP (5 mM) in the presence (blue bars) or absence (red bars) of Hsc70 (0.167 μM) and Hdj2 (0.167 μM) for 90 min at 25°C. Values represent means ± SEM (n = 4).

might also profoundly activate Hsp104 (Henriksen *et al.* 2012; Swaney *et al.* 2013; Weinert *et al.* 2013).

Understanding exactly how potentiated Hsp104 activity may be elicited and silenced by post-translational modifications might also help inform therapeutic strategies based on introduction of exogenous Hsp104 into degenerating neurons (Vacher, Garcia-Oroz and Rubinsztein 2005; Perrin *et al.* 2007; Lo Bianco *et al.* 2008; Vashist, Cushman and Shorter 2010; Cushman-Nick, Bonini and Shorter 2013). For example, it would likely be beneficial to reduce expression or activity of a therapeutic disaggregase after it has remediated the deleterious misfolding driving neurodegeneration. In this way, any toxic side effects of the disaggregase that might occur after misfolding is corrected could be avoided (Mack and Shorter 2016; Shorter 2016; Jackrel and Shorter 2017; Shorter 2017; Yasuda *et al.* 2017). A potential method to achieve this goal of tunable activity would be to synchronize the activity of the disaggregase based on the level of stress-signaling output of degenerating neurons. For example, Cdk5, a predominantly neural kinase exhibits hyperactive activity in degenerating neurons in various disorders (Su and Tsai 2011; Cheung and Ip 2012). Engineering Hsp104 with a Cdk5 consensus site at T499 or S535 could enable enhanced disaggregase activity elicited by phosphorylation by Cdk5, which would then decline upon restoration of proteostasis, mitigation of degeneration, and return of Cdk5 activity to normal levels. Variations on this theme that involve kinases other than Cdk5 or other reversible post-translational modifications can also be readily envisioned. In this way, enhanced disaggregase activity could be tuned via post-translational modification to suit the exact needs of the neuron.

We close with an important caveat. The phosphomimetic mutations in Hsp104 studied here may not accurately mimic phosphorylation of T499 or S535. In many cases, phosphomimetic mutations accurately phenocopy serine and threonine phosphorylation events and have been extremely informative (Lowe *et al.* 1998; Buck *et al.* 1999; Vitari *et al.* 2005; McKay and Morrison 2007; Truman *et al.* 2012; Dephoure *et al.* 2013). Indeed, phosphorylation sites often evolve from ancestral aspartate or glutamate residues (Pearlman, Serber and Ferrell 2011). However, in some cases, phosphomimetic mutations have not accurately represented the effects of phosphoserine or phosphothreonine (Dirac-Svejstrup *et al.* 2000; Paleologou *et al.* 2010; Hart and Vogt 2011; Dephoure *et al.* 2013; Skinner *et al.* 2017). Indeed, the size of the ionic shell and the negative charge of the phosphate group are different than aspartate or glutamate (Hunter 2012). Thus, phosphoserine or phosphothreonine creates a distinctive chemical microenvironment that is imperfectly mimicked by aspartate or glutamate (Hunter 2012). Consequently, it will be important to determine the activity of Hsp104 with phosphothreonine at position 499 or phosphoserine at position 535. Advances in technology to selectively incorporate non-natural amino acids, such as phosphoserine and phosphothreonine, into proteins are now available, which will enable general methods to biosynthesize defined phosphorylated versions of Hsp104 and indeed any specific phosphoprotein (Rogerson *et al.* 2015; Zhang *et al.* 2017).

Acknowledgement

We dedicate this paper to the memory of our mentor, advocate, hero, and friend Susan Lindquist. We thank Zach March for comments on the manuscript.

Funding

M.P.T. was supported by PENN-PORT Postdoctoral Fellowship K12GM081259 and K22NS09131401 NIH, K.L.M. was supported by an NSF graduate research fellowship (DGE-1321851), M.E.J. was supported by an AHA post-doctoral fellowship and a Target ALS Springboard Award, J.S. was supported by NIH grants (DP2OD002177, R01GM099836), a Muscular Dystrophy Association Research Award (MDA277268), the Life Extension Foundation, a Linda Montague Pechinik Research Award, the Packard Center for ALS Research at Johns Hopkins University, and Target ALS.

Conflict of interest. None declared.

REFERENCES

Abeliovich A, Gitler AD. Defects in trafficking bridge Parkinson's disease pathology and genetics. *Nature* 2016;**539**:207–16.

Albuquerque CP, Smolka MB, Payne SH *et al.* A multidimensional chromatography technology for in-depth phosphoproteome analysis. *Mol Cell Proteomics* 2008;**7**:1389–96.

Armakola M, Higgins MJ, Figley MD *et al.* Inhibition of RNA lariat debranching enzyme suppresses TDP-43 toxicity in ALS disease models. *Nat Genet* 2012;**44**:1302–9.

Downloaded from https://academic.oup.com/femsyr/article-abstract/18/5/foy042/4969683 by Washington University School of Medicine Library user on 04 January 2019

Auburger G, Sen NE, Meierhofer D *et al*. Efficient prevention of neurodegenerative diseases by depletion of starvation response factor Ataxin-2. *Trends Neurosci* 2017;**40**:507–16.

Auluck PK, Caraveo G, Lindquist S. Alpha-Synuclein: membrane interactions and toxicity in Parkinson's disease. *Annu Rev Cell Dev Biol* 2010;**26**:211–33.

Barmada SJ, Ju S, Arjun A *et al*. Amelioration of toxicity in neuronal models of amyotrophic lateral sclerosis by hUPF1. *Proc Natl Acad Sci USA* 2015;**112**:7821–6.

Becker LA, Huang B, Bieri G *et al*. Therapeutic reduction of ataxin-2 extends lifespan and reduces pathology in TDP-43 mice. *Nature* 2017;**544**:367–71.

Brettschneider J, Del Tredici K, Lee VM *et al*. Spreading of pathology in neurodegenerative diseases: a focus on human studies. *Nat Rev Neurosci* 2015;**16**:109–20.

Buck M, Poli V, van der Geer P *et al*. Phosphorylation of rat serine 105 or mouse threonine 217 in C/EBP beta is required for hepatocyte proliferation induced by TGF alpha. *Mol Cell* 1999;**4**:1087–92.

Caraveo G, Auluck PK, Whitesell L *et al*. Calcineurin determines toxic versus beneficial responses to alpha-synuclein. *Proc Natl Acad Sci* 2014;**111**:E3544–52.

Caraveo G, Soste M, Cappelleti V *et al*. FKBP12 contributes to alpha-synuclein toxicity by regulating the calcineurin-dependent phosphoproteome. *Proc Natl Acad Sci USA* 2017;**114**:E11313–E11322.

Cashikar AG, Duennwald M, Lindquist SL. A chaperone pathway in protein disaggregation. *J Biol Chem* 2005;**280**:23869–75.

Cashikar AG, Schirmer EC, Hattendorf DA *et al*. Defining a pathway of communication from the C-terminal peptide binding domain to the N-terminal ATPase domain in a AAA protein. *Mol Cell* 2002;**9**:751–60.

Castellano LM, Bart SM, Holmes VM *et al*. Repurposing Hsp104 to antagonize seminal amyloid and counter HIV infection. *Chem Biol* 2015;**22**:1074–86.

Chernoff YO, Lindquist SL, Ono B *et al*. Role of the chaperone protein Hsp104 in propagation of the yeast prion-like factor [psi+]. *Science* 1995;**268**:880–4.

Cheung ZH, Ip NY. Cdk5: a multifaceted kinase in neurodegenerative diseases. *Trends Cell Biol* 2012;**22**:169–75.

Chung CY, Khurana V, Auluck PK *et al*. Identification and rescue of alpha-synuclein toxicity in Parkinson patient-derived neurons. *Science* 2013;**342**:983–7.

Cooper AA, Gitler AD, Cashikar A *et al*. Alpha-synuclein blocks ER-Golgi traffic and Rab1 rescues neuron loss in Parkinson's models. *Science* 2006;**313**:324–8.

Cushman M, Johnson BS, King OD *et al*. Prion-like disorders: blurring the divide between transmissibility and infectivity. *J Cell Sci* 2010;**123**:1191–201.

Cushman-Nick M, Bonini NM, Shorter J. Hsp104 suppresses polyglutamine-induced degeneration post onset in a drosophila MJD/SCA3 model. *PLoS Genet* 2013;**9**:e1003781.

Daigle JG, Krishnamurthy K, Ramesh N *et al*. Pur-alpha regulates cytoplasmic stress granule dynamics and ameliorates FUS toxicity. *Acta Neuropathol* 2016;**131**:605–20.

Daigle JG, Lanson NA, Jr., Smith RB *et al*. RNA-binding ability of FUS regulates neurodegeneration, cytoplasmic mislocalization and incorporation into stress granules associated with FUS carrying ALS-linked mutations. *Hum Mol Genet* 2013;**22**:1193–205.

Dehay B, Bourdenx M, Gorry P *et al*. Targeting alpha-synuclein for treatment of Parkinson's disease: mechanistic and therapeutic considerations. *The Lancet Neurology* 2015;**14**:855–66.

Dephoure N, Gould KL, Gygi SP *et al*. Mapping and analysis of phosphorylation sites: a quick guide for cell biologists. *Mol Biol Cell* 2013;**24**:535–42.

DeSantis ME, Leung EH, Sweeny EA *et al*. Operational plasticity enables Hsp104 to disaggregate diverse amyloid and non-amyloid clients. *Cell* 2012;**151**:778–93.

DeSantis ME, Shorter J. The elusive middle domain of Hsp104 and ClpB: location and function. *Biochim Biophys Acta—Molecular Cell Res* 2012;**1823**:29–39.

DeSantis ME, Shorter J. Hsp104 drives "protein-only" positive selection of Sup35 prion strains encoding strong [PSI(+)]. *Chem Biol* 2012;**19**:1400–10.

DeSantis ME, Sweeny EA, Snead D *et al*. Conserved distal loop residues in the Hsp104 and ClpB middle domain contact nucleotide-binding domain 2 and enable Hsp70-dependent protein disaggregation. *J Biol Chem* 2014;**289**:848–67.

Dini Modigliani S, Morlando M, Errichelli L *et al*. An ALS-associated mutation in the FUS 3′-UTR disrupts a microRNA-FUS regulatory circuitry. *Nat Comms* 2014;**5**:4335.

Dirac-Svejstrup AB, Shorter J, Waters MG *et al*. Phosphorylation of the vesicle-tethering protein p115 by a casein kinase II-like enzyme is required for Golgi reassembly from isolated mitotic fragments. *J Cell Biol* 2000;**150**:475–88.

Duennwald ML, Echeverria A, Shorter J. Small heat shock proteins potentiate amyloid dissolution by protein disaggregases from yeast and humans. *PLoS Biol* 2012;**10**:e1001346.

Eisele YS, Monteiro C, Fearns C *et al*. Targeting protein aggregation for the treatment of degenerative diseases. *Nat Rev Drug Discov* 2015;**14**:759–80.

Elden AC, Kim HJ, Hart MP *et al*. Ataxin-2 intermediate-length polyglutamine expansions are associated with increased risk for ALS. *Nature* 2010;**466**:1069–75.

Gates SN, Yokom AL, Lin J *et al*. Ratchet-like polypeptide translocation mechanism of the AAA+ disaggregase Hsp104. *Science* 2017;**357**:273–9.

Gietz RD, Schiestl RH. High-efficiency yeast transformation using the LiAc/SS carrier DNA/PEG method. *Nat Protoc* 2007;**2**:31–34.

Gitcho MA, Bigio EH, Mishra M *et al*. TARDBP 3′-UTR variant in autopsy-confirmed frontotemporal lobar degeneration with TDP-43 proteinopathy. *Acta Neuropathol* 2009;**118**:633–45.

Gitler AD, Bevis BJ, Shorter J *et al*. The Parkinson's disease protein alpha-synuclein disrupts cellular Rab homeostasis. *Proc Natl Acad Sci* 2008;**105**:145–50.

Gitler AD, Chesi A, Geddie ML *et al*. Alpha-synuclein is part of a diverse and highly conserved interaction network that includes PARK9 and manganese toxicity. *Nat Genet* 2009;**41**:308–15.

Gitler AD, Shorter J. Prime time for alpha-synuclein. *J Neurosci* 2007;**27**:2433–4.

Glover JR, Lindquist S. Hsp104, Hsp70, and Hsp40. *Cell* 1998;**94**:73–82.

Guo L, Shorter J. Biology and pathobiology of TDP-43 and emergent therapeutic strategies. *Cold Spring Harb Perspect Med* 2017;**7**.

Halfmann R, Alberti S, Lindquist S. Prions, protein homeostasis, and phenotypic diversity. *Trends Cell Biol* 2010;**20**:125–33.

Harrison AF, Shorter J. RNA-binding proteins with prion-like domains in health and disease. *Biochem J* 2017;**474**:1417–38.

Hart JR, Vogt PK. Phosphorylation of AKT: a mutational analysis. *Oncotarget* 2011;**2**:467–76.

Harvey ZH, Chen Y, Jarosz DF. Protein-Based inheritance: Epigenetics beyond the chromosome. *Mol Cell* 2017;**69**:195–202.

Downloaded from https://academic.oup.com/femsyr/article-abstract/18/5/foy042/4969683 by Washington University School of Medicine Library user on 04 January 2019

Haslbeck M, Miess A, Stromer T *et al.* Disassembling protein aggregates in the yeast cytosol. *J Biol Chem* 2005;**280**:23861–8.

Haslberger T, Zdanowicz A, Brand I *et al.* Protein disaggregation by the AAA+ chaperone ClpB involves partial threading of looped polypeptide segments. *Nat Struct Mol Biol* 2008;**15**:641–50.

Henriksen P, Wagner SA, Weinert BT *et al.* Proteome-wide analysis of lysine acetylation suggests its broad regulatory scope in Saccharomyces cerevisiae. *Mol Cell Proteomics* 2012;**11**:1510–22.

Heuck A, Schitter-Sollner S, Suskiewicz MJ *et al.* Structural basis for the disaggregase activity and regulation of Hsp104. *Elife* 2016;**5**:e21516.

Holt LJ, Tuch BB, Villen J *et al.* Global analysis of Cdk1 substrate phosphorylation sites provides insights into evolution. *Science* 2009;**325**:1682–6.

Hunter T. Why nature chose phosphate to modify proteins. *Philos Trans R Soc B: Biol Sci* 2012;**367**:2513–6.

Jackrel ME, DeSantis ME, Martinez BA *et al.* Potentiated Hsp104 variants antagonize diverse proteotoxic misfolding events. *Cell* 2014;**156**:170–82.

Jackrel ME, Shorter J. Potentiated Hsp104 variants suppress toxicity of diverse neurodegenerative disease-linked proteins. *Dis Models Mech* 2014;**7**:1175–84.

Jackrel ME, Shorter J. Reversing deleterious protein aggregation with re-engineered protein disaggregases. *Cell Cycle* 2014;**13**:1379–83.

Jackrel ME, Shorter J. Engineering enhanced protein disaggregases for neurodegenerative disease. *Prion* 2015;**9**:90–109.

Jackrel ME, Shorter J. Protein-remodeling factors as potential therapeutics for neurodegenerative disease. *Front Neurosci* 2017;**11**:99.

Jackrel ME, Tariq A, Yee K *et al.* Isolating potentiated Hsp104 variants using yeast proteinopathy models. *J Vis Exp* 2014b;e52089, DOI: 10.3791/52089.

Jackrel ME, Yee K, Tariq A *et al.* Disparate mutations confer therapeutic gain of Hsp104 function. *ACS Chem Biol* 2015;**10**:2672–9.

Jarosz DF, Khurana V. Specification of physiologic and disease states by distinct proteins and protein conformations. *Cell* 2017;**171**:1001–14.

Johnson BS, McCaffery JM, Lindquist S *et al.* A yeast TDP-43 proteinopathy model: exploring the molecular determinants of TDP-43 aggregation and cellular toxicity. *Proc Natl Acad Sci* 2008;**105**:6439–44.

Johnson BS, Snead D, Lee JJ *et al.* TDP-43 is intrinsically aggregation-prone, and amyotrophic lateral sclerosis-linked mutations accelerate aggregation and increase toxicity. *J Biol Chem* 2009;**284**:20329–39.

Ju S, Tardiff DF, Han H *et al.* A yeast model of FUS/TLS-dependent cytotoxicity. *PLoS Biol* 2011;**9**:e1001052.

Kaimal JM, Kandasamy G, Gasser F *et al.* Coordinated Hsp110 and Hsp104 activities power protein disaggregation in Saccharomyces cerevisiae. *Mol Cell Biol* 2017;**37**:e00027–17.

Khurana V, Peng J, Chung CY *et al.* Genome-scale networks link neurodegenerative disease genes to alpha-synuclein through specific molecular pathways. *Cell Syst* 2017;**4**:157–170.e14, e14.

Kim HJ, Raphael AR, LaDow ES *et al.* Therapeutic modulation of eIF2alpha phosphorylation rescues TDP-43 toxicity in amyotrophic lateral sclerosis disease models. *Nat Genet* 2014;**46**:152–60.

King OD, Gitler AD, Shorter J. The tip of the iceberg: RNA-binding proteins with prion-like domains in neurodegenerative disease. *Brain Res* 2012;**1462**:61–80.

Klaips CL, Hochstrasser ML, Langlois CR *et al.* Spatial quality control bypasses cell-based limitations on proteostasis to promote prion curing. *Elife* 2014;**3**:e04288.

Kwiatkowski TJ, Jr., Bosco DA, Leclerc AL *et al.* Mutations in the FUS/TLS gene on chromosome 16 cause familial amyotrophic lateral sclerosis. *Science* 2009;**323**:1205–8.

Lagier-Tourenne C, Polymenidou M, Hutt KR *et al.* Divergent roles of ALS-linked proteins FUS/TLS and TDP-43 intersect in processing long pre-mRNAs. *Nat Neurosci* 2012;**15**:1488–97.

Lee J, Kim JH, Biter AB *et al.* Heat shock protein (Hsp) 70 is an activator of the Hsp104 motor. *Proc Natl Acad Sci* 2013;**110**:8513–8.

Lee T, Li YR, Chesi A *et al.* Evaluating the prevalence of polyglutamine repeat expansions in amyotrophic lateral sclerosis. *Neurology* 2011;**76**:2062–5.

Lee T, Li YR, Ingre C *et al.* Ataxin-2 intermediate-length polyglutamine expansions in European ALS patients. *Hum Mol Genet* 2011;**20**:1697–700.

Li YR, King OD, Shorter J *et al.* Stress granules as crucibles of ALS pathogenesis. *J Cell Biol* 2013;**201**:361–72.

Ling SC, Polymenidou M, Cleveland DW. Converging mechanisms in ALS and FTD: disrupted RNA and protein homeostasis. *Neuron* 2013;**79**:416–38.

Liu YH, Han YL, Song J *et al.* Heat shock protein 104 inhibited the fibrillization of prion peptide 106–126 and disassembled prion peptide 106–126 fibrils in vitro. *Int J Biochem Cell Biol* 2011;**43**:768–74.

Lo Bianco C, Shorter J, Regulier E *et al.* Hsp104 antagonizes α-synuclein aggregation and reduces dopaminergic degeneration in a rat model of Parkinson disease. *J Clin Invest* 2008;**118**:3087–97.

Lowe M, Rabouille C, Nakamura N *et al.* Cdc2 kinase directly phosphorylates the cis-Golgi matrix protein GM130 and is required for Golgi fragmentation in mitosis. *Cell* 1998;**94**:783–93.

Lum R, Niggemann M, Glover JR. Peptide and protein binding in the axial channel of Hsp104. *J Biol Chem* 2008;**283**:30139–50.

Lum R, Tkach JM, Vierling E *et al.* Evidence for an unfolding/threading mechanism for protein disaggregation by *Saccharomyces cerevisiae* Hsp104. *J Biol Chem* 2004;**279**:29139–46.

Mack KL, Shorter J. Engineering and evolution of molecular chaperones and protein disaggregases with enhanced activity. *Front Mol Biosci* 2016;**3**:8.

March ZM, King OD, Shorter J. Prion-like domains as epigenetic regulators, scaffolds for subcellular organization, and drivers of neurodegenerative disease. *Brain Res* 2016;**1647**:9–18.

McKay MM, Morrison DK. Integrating signals from RTKs to ERK/MAPK. *Oncogene* 2007;**26**:3113–21.

Neumann M, Sampathu DM, Kwong LK *et al.* Ubiquitinated TDP-43 in frontotemporal lobar degeneration and amyotrophic lateral sclerosis. *Science* 2006;**314**:130–3.

Newby GA, Lindquist S. Blessings in disguise: biological benefits of prion-like mechanisms. *Trends Cell Biol* 2013;**23**:251–9.

Outeiro TF, Lindquist S. Yeast cells provide insight into alpha-synuclein biology and pathobiology. *Science* 2003;**302**:1772–5.

Ovchinnikov S, Kamisetty H, Baker D. Robust and accurate prediction of residue–residue interactions across protein interfaces using evolutionary information. *Elife* 2014;**3**:e02030.

Paleologou KE, Oueslati A, Shakked G *et al.* Phosphorylation at S87 is enhanced in synucleinopathies, inhibits alpha-synuclein oligomerization, and influences synuclein-membrane interactions. *J Neurosci* 2010;**30**:3184–98.

Parsell DA, Kowal AS, Singer MA *et al.* Protein disaggregation mediated by heat-shock protein Hspl04. *Nature* 1994;**372**:475–8.

Downloaded from https://academic.oup.com/femsyr/article-abstract/18/5/foy042/4969683 by Washington University School of Medicine Library user on 04 January 2019

Parsell DA, Sanchez Y, Stitzel JD *et al.* Hspl04 is a highly conserved protein with two essential nucleotide-binding sites. *Nature* 1991;**353**:270–3.

Paushkin SV, Kushnirov VV, Smirnov VN *et al.* Propagation of the yeast prion-like [psi+] determinant is mediated by oligomerization of the SUP35-encoded polypeptide chain release factor. *EMBO J* 1996;**15**:3127–34.

Pearlman SM, Serber Z, Ferrell JE, Jr. A mechanism for the evolution of phosphorylation sites. *Cell* 2011;**147**:934–46.

Pei F, DiSalvo S, Sindi SS *et al.* A dominant-negative mutant inhibits multiple prion variants through a common mechanism. *PLoS Genet* 2017;**13**:e1007085.

Perrin V, Regulier E, Abbas-Terki T *et al.* Neuroprotection by Hsp104 and Hsp27 in lentiviral-based rat models of Huntington's disease. *Mol Ther* 2007;**15**:903–11.

Polymenidou M, Lagier-Tourenne C, Hutt KR *et al.* Long pre-mRNA depletion and RNA missplicing contribute to neuronal vulnerability from loss of TDP-43. *Nat Neurosci* 2011;**14**:459–68.

Rogerson DT, Sachdeva A, Wang K *et al.* Efficient genetic encoding of phosphoserine and its nonhydrolyzable analog. *Nat Chem Biol* 2015;**11**:496–503.

Sabatelli M, Moncada A, Conte A *et al.* Mutations in the 3′ untranslated region of FUS causing FUS overexpression are associated with amyotrophic lateral sclerosis. *Hum Mol Genet* 2013;**22**:4748–55.

Sanchez Y, Lindquist SL. HSP104 required for induced thermotolerance. *Science* 1990;**248**:1112–5.

Sanchez Y, Parsell DA, Taulien J *et al.* Genetic evidence for a functional relationship between Hsp104 and Hsp70. *J Bacteriol* 1993;**175**:6484–91.

Sanchez Y, Taulien J, Borkovich KA *et al.* Hsp104 is required for tolerance to many forms of stress. *EMBO J* 1992;**11**:2357–64.

Satyal SH, Schmidt E, Kitagawa K *et al.* Polyglutamine aggregates alter protein folding homeostasis in *Caenorhabditis elegans*. *Proc Natl Acad Sci* 2000;**97**:5750–5.

Schirmer EC, Homann OR, Kowal AS *et al.* Dominant gain-of-function mutations in Hsp104p reveal crucial roles for the middle region. *Mol Biol Cell* 2004;**15**:2061–72.

Shorter J. Hsp104: a weapon to combat diverse neurodegenerative disorders. *Neurosignals* 2008;**16**:63–74.

Shorter J. The mammalian disaggregase machinery: Hsp110 synergizes with Hsp70 and Hsp40 to catalyze protein disaggregation and reactivation in a cell-free system. *PLoS One* 2011;**6**:e26319.

Shorter J. Engineering therapeutic protein disaggregases. *Mol Biol Cell* 2016;**27**:1556–60.

Shorter J. Designer protein disaggregases to counter neurodegenerative disease. *Curr Opin Genet Dev* 2017;**44**:1–8.

Shorter J, Lindquist S. Hsp104 catalyzes formation and elimination of self-replicating Sup35 prion conformers. *Science* 2004;**304**:1793–7.

Shorter J, Lindquist S. Navigating the ClpB channel to solution. *Nat Struct Mol Biol* 2005;**12**:4–6.

Shorter J, Lindquist S. Prions as adaptive conduits of memory and inheritance. *Nat Rev Genet* 2005;**6**:435–50.

Shorter J, Lindquist S. Destruction or potentiation of different prions catalyzed by similar Hsp104 remodeling activities. *Mol Cell* 2006;**23**:425–38.

Shorter J, Lindquist S. Hsp104, Hsp70 and Hsp40 interplay regulates formation, growth and elimination of Sup35 prions. *EMBO J* 2008;**27**:2712–24.

Singleton AB, Farrer M, Johnson J *et al.* Alpha-Synuclein locus triplication causes Parkinson's disease. *Science* 2003;**302**:841.

Skinner JJ, Wang S, Lee J *et al.* Conserved salt-bridge competition triggered by phosphorylation regulates the protein interactome. *Proc Natl Acad Sci USA* 2017;**114**:13453–8.

Snead D, Eliezer D. Alpha-synuclein function and dysfunction on cellular membranes. *Exp Neurobiol* 2014;**23**:292–313.

Su LJ, Auluck PK, Outeiro TF *et al.* Compounds from an unbiased chemical screen reverse both ER-to-Golgi trafficking defects and mitochondrial dysfunction in Parkinson's disease models. *Dis Models Mech* 2010;**3**:194–208.

Su SC, Tsai LH. Cyclin-dependent kinases in brain development and disease. *Annu Rev Cell Dev Biol* 2011;**27**:465–91.

Sun Z, Diaz Z, Fang X *et al.* Molecular determinants and genetic modifiers of aggregation and toxicity for the ALS disease protein FUS/TLS. *PLoS Biol* 2011;**9**:e1000614.

Swaney DL, Beltrao P, Starita L *et al.* Global analysis of phosphorylation and ubiquitylation cross-talk in protein degradation. *Nat Methods* 2013;**10**:676–82.

Sweeny EA, Jackrel ME, Go MS *et al.* The Hsp104 N-terminal domain enables disaggregase plasticity and potentiation. *Mol Cell* 2015;**57**:836–49.

Sweeny EA, Shorter J. Prion proteostasis. *Prion* 2008;**2**:135–40.

Sweeny EA, Shorter J. Mechanistic and structural insights into the Prion-Disaggregase activity of Hsp104. *J Mol Biol* 2016;**428**:1870–85.

Tardiff DF, Jui NT, Khurana V *et al.* Yeast reveal a "druggable" Rsp5/Nedd4 network that ameliorates alpha-synuclein toxicity in neurons. *Science* 2013;**342**:979–83.

Tardiff DF, Lindquist S. Phenotypic screens for compounds that target the cellular pathologies underlying Parkinson's disease. *Drug Discov Today Technol* 2013;**10**:e121–8.

Tardiff DF, Tucci ML, Caldwell KA *et al.* Different 8-hydroxyquinolines protect models of TDP-43 protein, alpha-synuclein, and polyglutamine proteotoxicity through distinct mechanisms. *J Biol Chem* 2012;**287**:4107–20.

Tessarz P, Mogk A, Bukau B. Substrate threading through the central pore of the Hsp104 chaperone as a common mechanism for protein disaggregation and prion propagation. *Mol Microbiol* 2008;**68**:87–97.

Torrente MP, Chuang E, Noll MM *et al.* Mechanistic insights into Hsp104 potentiation. *J Biol Chem* 2016;**291**:5101–15.

True HL, Berlin I, Lindquist SL. Epigenetic regulation of translation reveals hidden genetic variation to produce complex traits. *Nature* 2004;**431**:184–7.

True HL, Lindquist SL. A yeast prion provides a mechanism for genetic variation and phenotypic diversity. *Nature* 2000;**407**:477–83.

Truman AW, Kristjansdottir K, Wolfgeher D *et al.* CDK-dependent Hsp70 Phosphorylation controls G1 cyclin abundance and cell-cycle progression. *Cell* 2012;**151**:1308–18.

Tuite MF, Serio TR. The prion hypothesis: from biological anomaly to basic regulatory mechanism. *Nat Rev Mol Cell Biol* 2010;**11**:823–33.

Vacher C, Garcia-Oroz L, Rubinsztein DC. Overexpression of yeast hsp104 reduces polyglutamine aggregation and prolongs survival of a transgenic mouse model of Huntington's disease. *Hum Mol Genet* 2005;**14**:3425–33.

Vance C, Rogelj B, Hortobagyi T *et al.* Mutations in FUS, an RNA processing protein, cause familial amyotrophic lateral sclerosis type 6. *Science* 2009;**323**:1208–11.

Vashist S, Cushman M, Shorter J. Applying Hsp104 to protein-misfolding disorders. *Biochem Cell Biol* 2010;**88**:1–13.

Vitari AC, Deak M, Morrice NA *et al.* The WNK1 and WNK4 protein kinases that are mutated in Gordon's hypertension

Downloaded from https://academic.oup.com/femsyr/article-abstract/18/5/foy042/4969683 by Washington University School of Medicine Library user on 04 January 2019

syndrome phosphorylate and activate SPAK and OSR1 protein kinases. *Biochem J* 2005;**391**:17–24.

Wallace EW, Kear-Scott JL, Pilipenko EV *et al*. Reversible, specific, active aggregates of endogenous proteins assemble upon heat stress. *Cell* 2015;**162**:1286–98.

Weinert BT, Scholz C, Wagner SA *et al*. Lysine succinylation is a frequently occurring modification in prokaryotes and eukaryotes and extensively overlaps with acetylation. *Cell Reports* 2013;**4**:842–51.

Wendler P, Shorter J, Snead D *et al*. Motor mechanism for protein threading through Hsp104. *Mol Cell* 2009;**34**:81–92.

Winner B, Jappelli R, Maji SK *et al*. In vivo demonstration that alpha-synuclein oligomers are toxic. *Proc Natl Acad Sci* 2011;**108**:4194–9.

Yasuda K, Clatterbuck-Soper SF, Jackrel ME *et al*. FUS inclusions disrupt RNA localization by sequestering kinesin-1 and inhibiting microtubule detyrosination. *J Cell Biol* 2017;**216**:1015–34.

Yokom AL, Gates SN, Jackrel ME *et al*. Spiral architecture of the Hsp104 disaggregase reveals the basis for polypeptide translocation. *Nat Struct Mol Biol* 2016;**23**:830–7.

Yu Z, Zhu Y, Chen-Plotkin AS *et al*. PolyQ repeat expansions in ATXN2 associated with ALS are CAA interrupted repeats. *PLoS One* 2011;**6**:e17951.

Zhang MS, Brunner SF, Huguenin-Dezot N *et al*. Biosynthesis and genetic encoding of phosphothreonine through parallel selection and deep sequencing. *Nat Meth* 2017;**14**:729–36.

Zhao X, Rodriguez R, Silberman RE *et al*. Heat shock protein 104 (Hsp104)-mediated curing of [PSI+] yeast prions depends on both [PSI+] conformation and the properties of the Hsp104 homologs. *J Biol Chem* 2017;**292**:8630–41.

Downloaded from https://academic.oup.com/femsyr/article-abstract/18/5/foy042/4969683 by Washington University School of Medicine Library user on 04 January 2019